

## Original Article



## *In vitro* and *In vivo* Evaluation of the Developed PLGA/HAp/Zein Scaffolds for Bone-Cartilage Interface Regeneration\*

LIN Yong Xin<sup>1,^</sup>, DING Zhi Yong<sup>2,^</sup>, ZHOU Xiao Bin<sup>1</sup>, LI Si Tao<sup>3</sup>,  
XIE De Ming<sup>4</sup>, LI Zhi Zhong<sup>1</sup>, and SUN Guo Dong<sup>1,#</sup>

1. Department of Orthopedics, the First Affiliated Hospital of Jinan University, Guangzhou 510630, Guangdong, China; 2. Department of Traumatology, HuiZhou Municipal Central Hospital, Huizhou 516000, Guangdong, China; 3. Department of Pediatrics, the Sixth Affiliated Hospital of Sun Yat-sen University, Guangzhou 510655, Guangdong, China; 4. Department of Biomedical Engineering, College of Life Science and Technology, Jinan University, Guangzhou 510630, Guangdong, China

### Abstract

**Objective** To investigate the effect of electrospun PLGA/HAp/Zein scaffolds on the repair of cartilage defects.

**Methods** The PLGA/HAp/Zein composite scaffolds were fabricated by electrospinning method. The physiochemical properties and biocompatibility of the scaffolds were separately characterized by scanning electron microscope (SEM), transmission electron microscope (TEM), and fourier transform infrared spectroscopy (FTIR), human umbilical cord mesenchymal stem cells (hUC-MSCs) culture and animal experiments.

**Results** The prepared PLGA/HAp/Zein scaffolds showed fibrous structure with homogenous distribution. hUC-MSCs could attach to and grow well on PLGA/HAp/Zein scaffolds, and there was no significant difference between cell proliferation on scaffolds and that without scaffolds ( $P>0.05$ ). The PLGA/HAp/Zein scaffolds possessed excellent ability to promote *in vivo* cartilage formation. Moreover, there was a large amount of immature chondrocytes and matrix with cartilage lacuna on PLGA/HAp/Zein scaffolds.

**Conclusion** The data suggest that the PLGA/HAp/Zein scaffolds possess good biocompatibility, which are anticipated to be potentially applied in cartilage tissue engineering and reconstruction.

**Key words:** hUC-MSCs; Electrospun; PLGA/HAp/Zein grafts; Cartilage tissue engineering; Chondrocyte

*Biomed Environ Sci*, 2015; 28(1): 1-12

doi: 10.3967/bes2015.001

ISSN: 0895-3988

[www.besjournal.com](http://www.besjournal.com) (full text)

CN: 11-2816/Q

Copyright ©2015 by China CDC

### INTRODUCTION

Osteoarthritis (OA) is a major cause of pain and disability in the aging population<sup>[1]</sup>, which mainly invades

articular cartilage, bone and synovial tissue and induces joint pain, deformity and dysfunction. As is known, the cartilage self-healing is limited due to the lack of blood supply, nerve and lymphoid tissue. Thus, regeneration of articular cartilage, also known

\*This research was financially supported by the National Natural Science Foundation of China, No. 31070862; Science and Technology Plan of Guangzhou, No. 12C32071662; Research Foundation of Guangdong Provincial Bureau of Traditional Chinese Medicine, No. 2013113; scientific research and cultivating Foundation of the First Clinical Medical College of Jinan University, No. 2012103 and No. 2013208.

<sup>^</sup>These authors contributed equally to this work.

<sup>#</sup>Correspondence should be addressed to SUN Guo Dong, Tel: 86-20-3868-8617, Fax: 86-20-3868-8619, E-mail: [sunguodongjn@163.com](mailto:sunguodongjn@163.com)

Biographical notes of the first authors: LIN Yong Xin, male, born in 1965, majoring in spine surgery and tissue engineering; DING Zhi Yong, male, born in 1986, majoring in spine surgery and tissue engineering.

as hyaline cartilage, is one of the most critical challenges in arthritis, joint disorders and trauma<sup>[2-3]</sup>.

Over the past two decades, tissue engineering research has made considerable progress because of the rapid development of bioengineering and biotechnology<sup>[4-6]</sup>. For the reconstruction of tissue engineering bone-cartilage, the selection of appropriate scaffolds is key to determining the outcome of reconstruction. Scaffold architecture and composition are important parameters in cartilage tissue engineering<sup>[7]</sup>. In terms of three-dimensionality, chondrocytes are arrested to 3D-scaffolds for implantation<sup>[7]</sup>. In most cases, the scaffold characteristics will greatly influence cells attachment, morphology and proliferation, and thus scaffolds should be designed to mimic the complex micro-environment for promoting tissue regeneration<sup>[8]</sup>. In recent years, the synthetic polymers have been widely used in various tissue engineering fields due to their excellent biomechanics, biodegradability and biocompatibility. Poly (lactide-co-glycolide) (PLGA) is a FDA approved synthetic biomaterial that has been applied to the regenerative medicine due to its superiority in all the aforementioned properties. PLGA has also been used extensively in preclinical studies of ligament, tendon and cartilage, as well as in bone regenerative medicine<sup>[9]</sup>. The PLGA scaffolds are porous and suitable for the attachment, proliferation and differentiation of cells without affecting their morphology and growth. Moreover, the scaffolds possess better mechanical property and are readily fabricated. Thus, PLGA is the most widely used biodegradable materials<sup>[10]</sup>. However, PLGA has poor hydrophilicity, and PLGA molecular chains are in lack of bioactive groups, therefore, it is very difficult for PLGA to interact with specific cells<sup>[11-12]</sup> by itself. Hydroxyapatite (HAp) has good hydrophilicity and bioactivity, and has been widely used for bone repair and tissue engineering<sup>[13]</sup>, but its mechanical property is poor, such as low intensity, poor toughness and large brittleness. Moreover, HAp is easy to be fatigued and damaged under physiological conditions. Zein has been extensively used in a wide range of tissue engineering and drug delivery system due to its good cell compatibility<sup>[14-15]</sup>. It was reported that a three-dimensional Zein porous scaffold could promote the adhesion, proliferation and osteogenic differentiation of rat mesenchymal stem cells (MSCs). Moreover, the highly porous Zein scaffolds showed improved mechanical properties, which might be

applied as bone-cartilage substitution<sup>[16]</sup>. In addition, the Zein porous scaffold was also found to have good tissue compatibility *in vivo*<sup>[17]</sup>. Therefore, the addition of Zein in our study was anticipated to further promote the formation of bone tissue due to its good biocompatibility, osteogenic activity, biodegradation property, and vasoactivity<sup>[18]</sup>. Thus, based on the above knowledge, combining PLGA, and HAp by a suitable method may form an ideal tissue engineering scaffold for cartilage repair.

In this study, the PLGA/HAp/Zein scaffolds for bone-cartilage tissue engineering were prepared using electrospinning method. The physiochemical properties of the scaffolds were characterized by SEM, TEM, and FTIR, and their biocompatibility was evaluated using hUC-MSCs *in vitro*. Subsequently, the *in vivo* animal experiment was performed to further evaluate the biocompatibility of the PLGA/HAp/Zein scaffolds, and the effect of the scaffolds on cartilage reconstruction was discussed.

## MATERIALS AND METHODS

### *Materials and Reagents*

New Zealand rabbits (total number: 60, 3-4 months), female or male with the weight of 2.1-3.2 kg (average weight: 2.5 kg) were supplied by Guangdong experimental center. The umbilical cords from healthy full-term cesarean mothers were provided by obstetricians in the First Affiliated Hospital of Jinan University (with consent by their families and approval by the ethics committee in hospital). Collagenase (type II), 3-(4, 5-Dimethylthiazol-2-yl)-2, 5-diphenyltetrazolium bromide (MTT) and CK-150 high speed centrifuge were from Sigma Aldrich (USA). Fetal bovine serum was purchased from Gibco, Uruguay. The mouse anti-human antibody labeled by fluorescence was from BD Pharmingen, USA, Trypsin/EDTA and green streptomycin were both supplied by TBD, USA. CO<sub>2</sub> incubator was from Thermo Forma, USA. The inverted phase contrast microscope was from Olympus, Japan. The flow cytometer was purchased from Coulter-Elite, USA, and the automatic microplate reader was obtained from Bio-Rad, USA. All the other reagents used in the experiments were of the highest analytical purity (>99.9%).

### *Fabrication of PLGA/HAp/Zein Scaffolds*

Firstly, the nano HAp with different mass was dispersed in hexafluoroisopropanol (HFIP) solvent by

stirring overnight, and thus the HAp suspension with various concentrations was obtained. Then a certain amount of PLGA was diluted in HAp suspension, stirred until the nano HAp dispersed thoroughly in PLGA solution. Subsequently, Zein was added to the above PLGA solution and diluted and mixed completely. Thereafter, the HAp concentration was adjusted to 35%, and the Zein concentration was adjusted to 35% and 60%, respectively. Finally, the spinning parameters of the electrostatic spinning apparatus were adjusted, so that the PLGA solution containing HAp with different concentrations could be successfully spun out. The receiving board was standing statically and the parameters for electrospun were listed in Table 1.

### **Physicochemical Characterization of PLGA/HAp/Zein Scaffolds**

The scaffolds together with the collecting aluminum sheet were cut into small pieces of 5 mm×5 mm. Then the scaffolds were carefully peeled off from the aluminum sheet using ophthalmic tweezers, and flattened on the slide after having been wetted with PBS. The general morphology of the scaffolds was observed using an inverted microscope, and then the scaffolds were freeze-dried and coated with gold, the micro-morphology was observed by SEM (Philips, Netherland). In addition, the surface morphology of the single spun Zein film was also detected by SEM as a control. For the analysis of the internal structure of the fiber, the copper mesh was used to collect single or several PLGA/HAp/Zein fibers, and then the dispersion of HAp nanoparticles was observed by TEM (JEM-0360LV, Japan). The FTIR of the pure Zein, PLGA/Hap electrospun film, PLGA/HAp/Zein electrospun film was obtained from a FTIR spectrometer (EQUINOX55, Bruker). For each spectrum obtained, a total of 64 scans were accumulated at 2 cm<sup>-1</sup> resolution. Scanning was conducted in the range from 400 to 4000 cm<sup>-1</sup>.

### **Isolation and Identification of hUC-MSCs**

The sterile umbilical cord tissue (about 10 cm and close to the fetal side) from healthy full-term births

was taken from the operating room (according to the hospital regulations and with the consent of their families). And then the tissue was immersed into PBS containing 10% green streptomycin at 4 °C and used within 6 h. Subsequently, the two ends of the umbilical cord were cut off in a clean bench (about 5 cm left), and washed with PBS containing 1% green streptomycin by a syringe in order to remove the residual blood. The outer membrane and blood vessels were peeled off, thus, the Wharton tissue was obtained. Then the Wharton tissue was cut into small pieces of 1 mm<sup>3</sup>, immersed in 20 mL 0.1% collagenase (type II) and digested at 37 °C in an air shaker with 200 rpm for 6 h. Subsequently, the digest was filtered, collected and centrifuged at 3000 rpm for 10 min at room temperature, the supernatant was dropped while the precipitation was retained and rinsed with PBS twice. Then the LG/DMEM/F12 medium with 10% FBS was added and cultured in a 25 cm<sup>2</sup> flask with the concentration of 1×10<sup>6</sup> cells/mL. The culture was performed in an incubator with 5% CO<sub>2</sub> at 37 °C. After 6-7 d of culture, the original medium was first changed with the new medium for removing the dead and hybrid cells, and then the medium was changed every 3-4 d until a 80% of cell confluence was reached. Thereafter, the cells were digested with 0.25% trypsin for 3-5 min and subcultured (1:3). The morphological change and proliferation of the cells were observed using an inverted microscope during these processes.

The surface specific antigen of the 3rd generation of hUC-MSCs was detected by flow cytometry as follows: the cells were trypsinized using 0.25% trypsin and washed with PBS for three times, and thus the cell suspension with 1×10<sup>6</sup> cells/mL was obtained. Then the first antibodies were added to 0.1 mL cell suspension and incubated at 4 °C for 30 min. Subsequently, the second antibodies labeled with fluorescence were added and incubated at 4 °C for 30 min. Finally, the cells were fixed with 100 mL/L formalin and the positive ratios of various antigens were measured by flow cytometry.

### **Culture of hUC-MSCs on PLGA/HAp/Zein Scaffolds**

The scaffolds together with the collecting aluminum sheet were cut into small pieces of 5 mm×5 mm and irradiated using ultraviolet. Then the scaffolds were carefully peeled off from the aluminum sheet using ophthalmic tweezers and placed into the 96-well plate after having been rinsed by PBS. After digesting hUC-MSCs by 0.25%

**Table 1.** The Parameters for Electrospun of PLGA/HAp/Zein Scaffolds

Parameter	Value
Voltage	20-25 kv
Solution flow rate	1.5-2.0 mL/h
Needle diameter	0.8 mm
Spinning distance	15 cm

trypsin/0.05% EDTA, the cell concentration was adjusted to  $1.5 \times 10^4$  cells/mL. And then 200  $\mu$ L cell suspension was added to the wells of 96-well plate (three duplicate wells were used); in addition, the same volume of cell suspension was added to the control wells without PLGA/HAp/Zein scaffolds. Subsequently, the plate was incubated in an incubator with 5% CO<sub>2</sub> at 37 °C, the medium was changed every 3 d, and the attachment, spreading and proliferation of cells on the scaffolds were observed by an inverted microscope. After culture for 1, 3, and 5 d, respectively, the samples were fixed with 2.5% glutaraldehyde, dehydrated with gradient alcohol, freeze dried. Finally, the cell morphology was observed by SEM after having been coated with gold.

#### **Proliferation and Doubling Time of hUC-MSCs by MTT**

After culture for 1, 3, 5, 7, and 9 d, respectively, the proliferation of hUC-MSCs in 96-well plate was detected using MTT assay. The experimental procedure was referring to the instruction of MTT kit. Briefly, MTT was dissolved in PBS to obtain a concentration of 5 mg/mL, and then MTT solution was added to each well (50  $\mu$ L/well) and incubated in an incubator with 5% CO<sub>2</sub> at 37 °C for 4 h. Subsequently, 150  $\mu$ L DMSO solution was added and shaking for 10 min. Finally, the optical density (OD) at 550 nm was determined by a microplate reader. For calculating the doubling time, the following equation can be used:

$$T_d = t \times [\lg 2 / (\lg N_t - \lg N_0)] \quad (1)$$

$T_d$  is doubling time,  $t$  is the culture time,  $N_0$  is the initial seeding concentration,  $N_t$  is the cell concentration after culture for  $t$  days.

#### **Cytotoxicity Test**

The standard concentration of material extracts is 10 mL/cm<sup>2</sup> (ratio of the medium volume to the material surface area). The sterile scaffolds were immersed in culture medium and incubated in an incubator (37 °C, 5% CO<sub>2</sub>) for 48 h, then the extracts were taken out and stored sterile at 4 °C before use. In addition, the extracts with 0.25 $\times$ , 0.5 $\times$ , 2 $\times$ , and 4 $\times$  were also prepared using the same method.

Then hUC-MSCs in the logarithmic growth phase were seeded in the 96-well plate ( $1.5 \times 10^4$  cells/mL, 200  $\mu$ L/well) and cultured for 4 h. Subsequently, the original medium was changed by the extracts and incubated for 1, 3, and 5 d, and the cells in DMEM/F12 were used as negative control. The cell

activity was detected by MTT assay as described above, and the relative growth ratio (RGR) of hUC-MSCs and cytotoxicity of the scaffolds were evaluated as follows:

$$RGR = (\text{OD value of the samples} / \text{OD value of the negative control}) \times 100\% \quad (2)$$

And the cytotoxicity was divided into five grades, grade 0: RGR  $\geq$  100%, grade 1: RGR  $\geq$  80%, grade 2: RGR  $\geq$  50%, grade 3: RGR  $\geq$  30%, grade 4: RGR  $\geq$  0. Only the materials with cytotoxicity between grade 0 and grade 1 could be used for *in vivo* experiments.

#### **Preparation of Cell-scaffold Complexes**

The scaffolds together with the collecting aluminum sheet were cut into small pieces of 1 cm  $\times$  1 cm and irradiated using ultraviolet for 1 h before use. Then the scaffolds were carefully peeled off from the aluminum sheet using ophthalmic tweezers and placed into the 6-well plate after having been rinsed by PBS. After digesting hUC-MSCs by 0.25% trypsin/0.05% EDTA, the cell concentration was adjusted to  $1 \times 10^6$  cells/mL. And then 2 mL cell suspension was added to the wells of 6-well plate and incubated in an incubator with 5% CO<sub>2</sub> at 37 °C for 3 h. Thereafter, 2 mL chondrogenic induction medium (with 1% FBS, 10  $\mu$ g/L TGF- $\beta$ 1, 6.25 mg/L transferrin, 6.25 mg/L insulin,  $10^{-7}$  mol/L dexamethasone, 50 mg/L vitamin C and DMEM induction medium with high glucose) was added to each well. The medium was changed every three days and the cells were used for *in vivo* experiments after culture for 7 d.

#### **Preparation and Grouping of Animal Model**

The rabbits in the experiment were divided into three groups, group A: cell-scaffold complexes, N=30; group B: single scaffold without cells, N=15, and group; C: blank control, N=15. Anesthesia and pre-surgical preparation: All rabbits were weighed and injected intramuscularly with penicillin of 400,000 units, and anesthetized by ear vein injection with 3% sodium pentobarbital (30 mg/kg). Then the rabbit limbs were fixed by the prone position, sheared at knees, and sterilized using 5% iodophor. Surgical steps<sup>[19-20]</sup>: the drill and tap were used to penetrate into the knee from the lateral margin of patella to expose the femoral surface. And then a defect with diameter of 5 mm and depth of 3 mm was fabricated on the femoral surface, and during this process the subchondral bone should not be damaged. In addition, the bone chips were removed using physiological saline and the blood was blocked

by plugging dry gauze. For group A, the cell-scaffold complexes were implanted into the right side of femoral condyle of each rabbit. For group B, the single scaffold without cells was implanted into the left side of femoral condyle of 15 rabbits, respectively. And for group C, no scaffold was implanted into the left side of femoral condyle of the remaining 15 rabbits. The sarcolemma, fascia and skin were sutured using silk (7#), then the animals were raised in different cages and were injected intramuscularly with penicillin of 400,000 units within 3 d before and after the surgery.

### **Morphological Observation**

Firstly, the diet, activity, wound swelling and exudation of the animals after surgery were monitored. Then after 6 weeks of surgery, the rabbits were killed by injecting air to the ear vein. The knees were opened and the patellar ligament was crosscut, then the joint capsule was opened and the femur bottom was exposed<sup>[20-21]</sup>. Thus, the general observation could be performed. Subsequently, the soft tissue was removed and the bone was taken out, then the histological analysis was performed as follows: the samples were fixed in 4% polyformaldehyde for 48 h and decalcified in saturated EDTA-Na solution until the calcium was removed completely, and the EDTA-Na solution was changed every 3 d. Then the samples were dehydrated using ethanol and immersed into dimethylbenzene to make the tissue transparent. Subsequently, the samples were embedded using paraffin and sliced to the thickness of 5  $\mu\text{m}$ . Finally, the slices were stained using hematoxylin and eosin (HE) and observed by an inverted microscope.

### **Data Analysis**

The data were analyzed with the software SPSS 17.0 (Chicago, Illinois). Statistical evaluation of the data was performed using one way ANOVA analysis. The probability ( $P$ ) values  $P < 0.05$  were considered to be statistically significant differences. The results were expressed as mean  $\pm$  standard deviation (SD).

## **RESULTS**

### **Physicochemical Characterization of PLGA/HAp/Zein Scaffolds**

The feasibility of electrospinning Zein was first studied. After stirring for a 5 min, Zein could be dissolved well in HFIP. Then the solubility of Zein in

HFIP was adjusted, and it was found that Zein with 4-22 wt% in HFIP could be spun well, while Zein with too high or too low concentration was difficult to be spun out. Figure 1 shows the SEM and TEM results of the electrospun scaffolds. It could be seen from Figure 1A that there were plenty of random fibers in the spun Zein, and the diameter of most of the fibers was within 1  $\mu\text{m}$ . Thus, when the Zein solution was spouted to the collecting device, the solution was still in wet status due to the uncompleted evaporation of the solvent. In addition, the tensile force on fibers from the electric field disappeared during the spout process. Thus, the fiber would be relaxed due to the effect of surface tension and viscoelasticity of the polymer solution, and the beads were formed. Both the PLGA and Zein could be diluted by HFIP solvent, but when they were together diluted in HFIP, the phase separation would appear after remaining stationary at room temperature overnight, which might be associated with their different polarity. However, when PLGA was blended with 35% Zein, the spinning could be performed well without phase separation. Moreover, an uniform size of the fiber size was obtained (Figure 1B). Subsequently, after further addition of 35% HAp, the morphology of the scaffolds (Figure 1C) showed virtually no obvious difference compared with that in Figure 1B, indicating that the addition of Zein did not affect the spinning of the scaffolds, and the diameter of the fibers was still in the range between 200 nm and 2  $\mu\text{m}$ . Nevertheless, after further increasing the concentration of Zein to 60%, a small amount of beads appeared again (Figure 1D). Thus, the PLGA/HAp/Zein scaffolds with 35% HAp and 35% Zein were mainly used in our following study. The SEM findings indicated that the PLGA/HAp/Zein scaffolds with better morphology could be successfully prepared by electrospun method.

Then, TEM was used to further observe the morphology of the prepared PLGA/HAp/Zein scaffolds. As shown in Figure 1E, the fiber surface of PLGA+35% Zein was smooth and the fiber diameter was in the range between 200 and 300 nm, which was similar to the diameter of the single electrospun PLGA fiber. Then after adding HAp nanoparticles, the fiber diameter increased to the range of 200-500 nm. And most of the particles distributed evenly in the inner and outer surface of the fiber, but few nanoparticles were clustered on the surface of the fiber (Figure 1F). After further increasing the concentration of Zein, there was no obvious difference in the fiber diameter and the distribution

of HAp nanoparticles (Figure 1G) compared with Figure 1F.

In addition, the FTIR analysis was used for further characterizing the electrospun PLGA/HAp/Zein scaffolds (Figure 2). The FTIR spectra of PLGA/HAp scaffolds showed that the peaks of  $\text{PO}_4^{3-}$  groups in 570, 600, 960, and 1030  $\text{cm}^{-1}$  were covered by the PLGA peaks, while the  $-\text{OH}$  peaks in 3400  $\text{cm}^{-1}$  were increased obviously. The FTIR spectra of PLGA/Zein scaffolds exhibited that the characteristic peaks of amide I ( $\text{C}=\text{O}$ ) and amide II ( $\text{N}-\text{H}$ ) of Zein appeared in 1650-1655  $\text{cm}^{-1}$  and 1539-1545  $\text{cm}^{-1}$ , respectively. Subsequently, after the electrospun PLGA/HAp/Zein scaffolds was formed, the peaks of amide I and amide II were decreased, but the  $\text{C}=\text{O}$  peaks in 1800  $\text{cm}^{-1}$ ,  $\text{C}-\text{O}$  peaks in 1188  $\text{cm}^{-1}$ , and  $-\text{OH}$  stretch vibration in 1200  $\text{cm}^{-1}$  were obvious. However, as is known, these three characteristic peaks mainly appeared in FTIR spectra of PLGA or

HAp, and the reason for that might be ascribed to the small concentration of Zein in PLGA/HAp/Zein scaffolds. The detailed reason behind should be further elaborated in our future work. In addition, from the FTIR spectra of PLGA/Zein, it could be seen that there was no obvious chemical bond between the two materials, indicating a phase separation of the two component, and the results were consistent well with our above finding.

### **Morphological Observation and Determination of Surface Antigen Marker of hUC-MSCs**

After culture for 3 d of the primary cells, there were a few scattered cells with different morphological features including short spindle, spindle and flat polygonal (Figure 3A). On the 5<sup>th</sup> day of culture, the number of the cells increased obviously, and the cells mainly showed long spindle and flat polygonal morphology (Figure 3B), which was

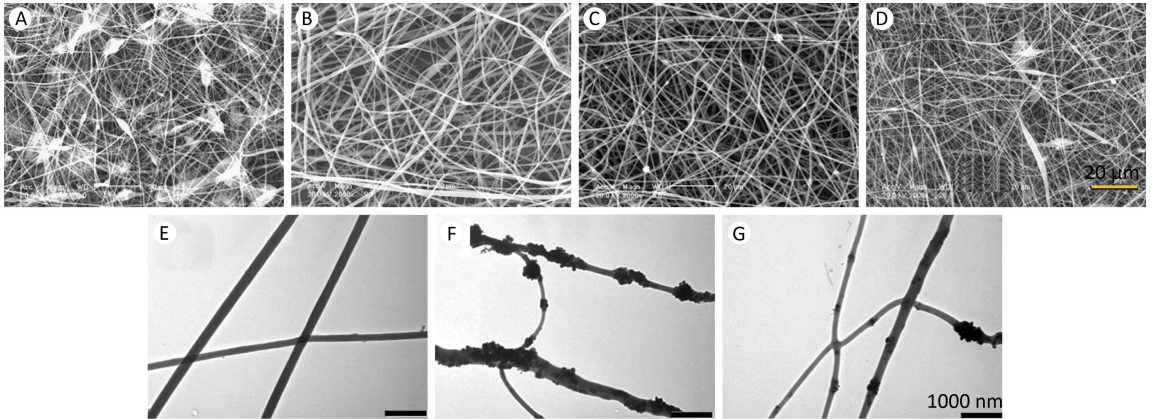


**Figure 1.** The representative SEM and TEM images of the prepared electrospun scaffolds. (A) Zein; (B, E) PLGA+35% Zein; (C, F) PLGA+35% HAp+35% Zein; (D, G) PLGA+35% HAp+60% Zein.

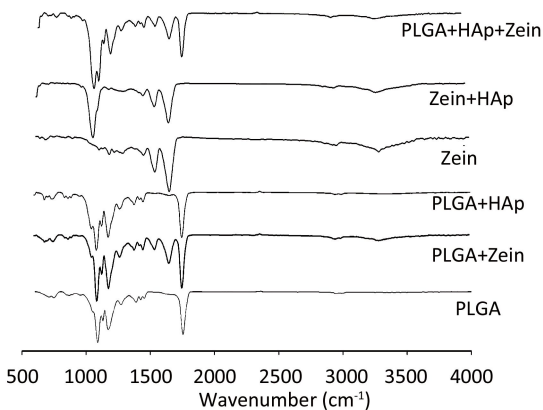


**Figure 2.** FTIR spectra of the electrospun scaffolds with different components.

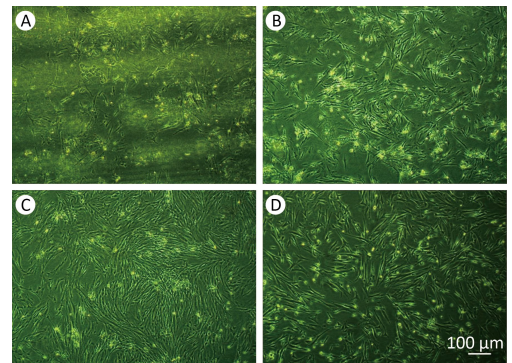


**Figure 3.** Morphology of hUC-MSCs by an inverted microscope. (A-C) the primary cells cultured for 3, 5, and 7 d, respectively ( $\times 40$ ); (D) the third passage of the cells after culture for 3 d ( $\times 40$ ).

similar to the typical morphology of fibroblasts. Then after further culture for 7 d, the cells covered the whole bottom of the flask and displayed swirling or radial morphology. Moreover, some cells were fused together with unclear cell gaps (Figure 3C). When the cells were subcultured to the third passage (P3), their viability was still very good after incubation for 3 d (Figure 3D). All the cells showed triangle or polygonal morphology with plump shape, and the secretion of extracellular matrix was increased.

The tests by flow cytometry in Figure 4 identified that the hUC-MSCs highly expressed MSC markers (CD105, CD90, CD73) and adhesion molecular markers (CD44, CD13, CD29), while not expressing hematopoietic stem cells markers (CD34, CD14, CD45, CD31, CD40) or MHC-II molecular markers (HLA-DR). Thus, the hUC-MSCs in our study were differentiation-specific and could be used for cartilage repair.

### Culture of hUC-MSCs on PLGA/HAp/Zein Scaffolds

The hUC-MSCs cultured on PLGA/HAp/Zein scaffolds for 1, 3, and 5 d were observed using SEM. As shown in Figure 5A, the cells were attached on the surface of the scaffolds, and a round morphology appeared after culture for 1 d. Then the number of cells increased after 3 d of culture, indicating an obvious cell proliferation, and an absence of cytotoxicity. And after culture for 5 d, the cells covered almost the whole surface of the scaffolds. Moreover, it could be seen clearly from the SEM images that the cells adhered on the fibers with multiple pseudopodia, which would be beneficial for the stability of hUC-MSCs on the scaffolds. The morphology of hUC-MSCs was consistent well with that reported by Shin et al.<sup>[22]</sup>. The PLGA/HAp/Zein scaffolds were found to be suitable for the growth and proliferation of hUC-MSCs.

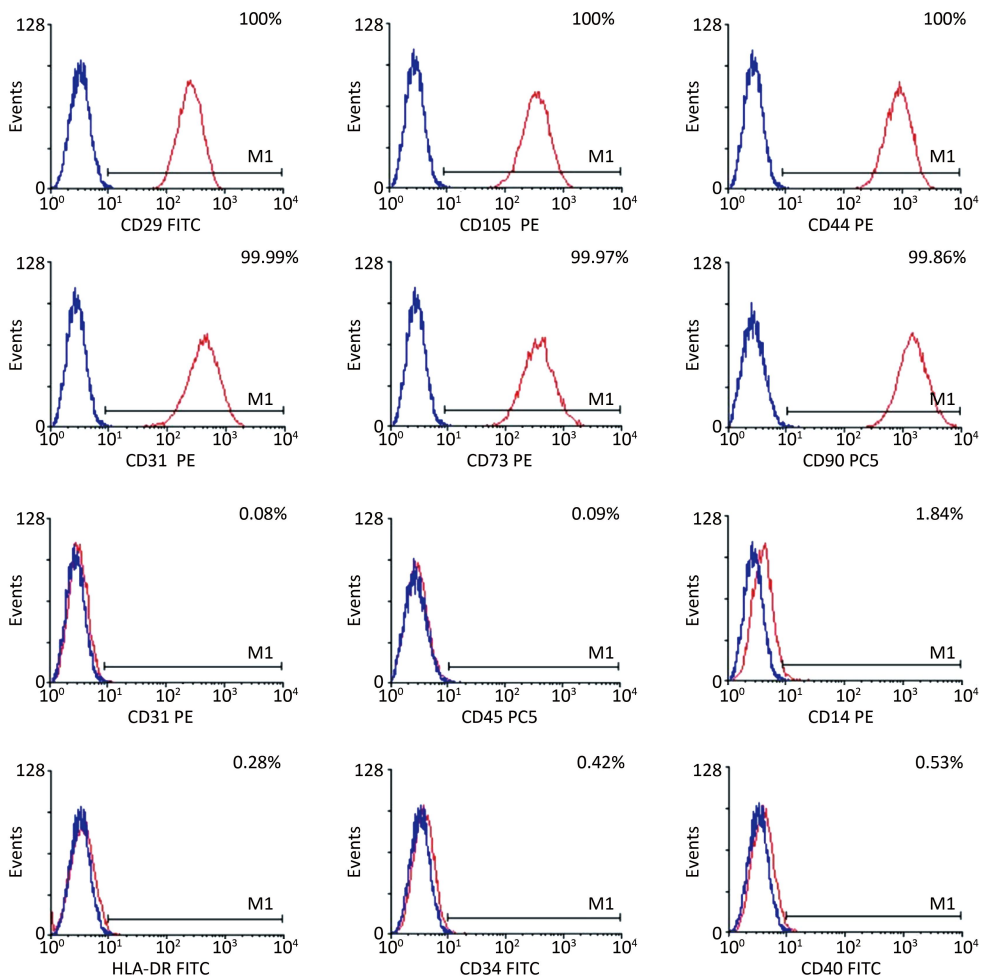


**Figure 4.** The surface markers of hUC-MSCs by flow cytometry.

In this study, the proliferation and doubling time of hUC-MSCs on PLGA/HAp/Zein scaffold and tissue culture plate were compared using MTT method. The comparison revealed that there was no obvious difference in the cell proliferation between the two groups (Figure 5B). On the first 3 d, the growth of hUC-MSCs was in the stagnation period, from the 4<sup>th</sup> to the 6<sup>th</sup> day, the cells were in logarithmic growth phase, and then after 7 d of culture, the cells were in a plateau period. In addition, the doubling time of hUC-MSCs on the scaffold and tissue culture plate was  $18.56 \pm 0.35$  h and  $19.73 \pm 0.24$  h, respectively, indicating no significant difference in the doubling time of hUC-MSCs between the two groups ( $P > 0.05$ ). Moreover, the PLGA/HAp/Zein scaffold possessed good cytocompatibility, which was consistent well with the above results.

### Cytotoxicity test of PLGA/HAp/Zein Scaffolds

Table 2 shows the cytotoxicity of PLGA/HAp/Zein scaffolds by MTT test. The toxicity grades of various concentrations in different periods were all in the range from 0 to 1. The statistical analysis by SPSS 17.0 displayed that there was no significant difference in the OD values among the various concentrations on d 1, d 3, and d 5 ( $P > 0.05$ ). All the OD values were prolonged with the increased incubation time, indicating that the number of cells was increased with the incubation time. In addition, it was also noted that the effect of extracts with a high concentration on cell growth showed no obvious difference compared with the extracts at a low concentration ( $P > 0.05$ ). Therefore, the extracts PLGA/HAp/Zein scaffolds exhibited no cytotoxicity and

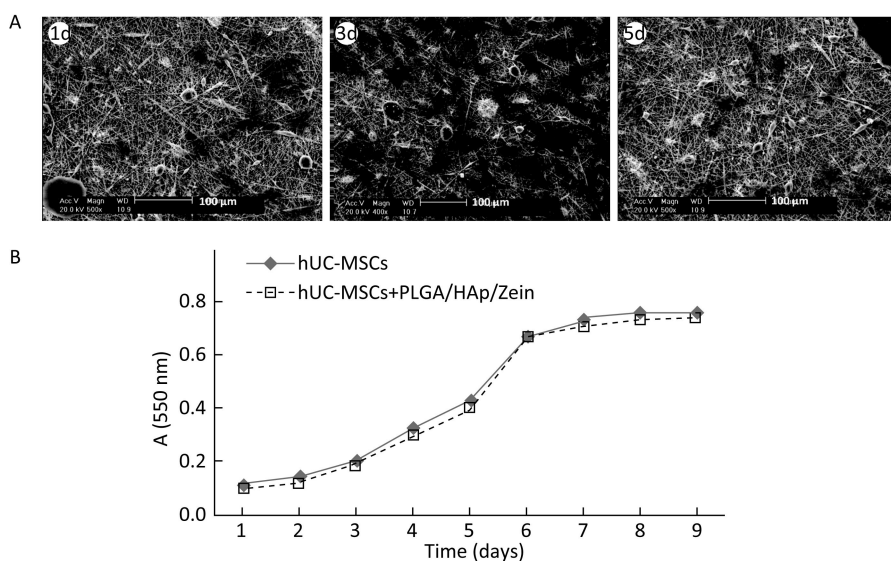


**Figure 5.** (A) The SEM images of hUC-MSCs cultured on PLGA/HAp/Zein scaffolds for 1, 3, and 5 d, respectively. And (B) the proliferation curves of hUC-MSCs on PLGA/HAp/Zein scaffolds by MTT assay.

**Table 2.** Cytotoxicity of PLGA/HAp/Zein Scaffolds by MTT

Group	1 d			3 d			5 d		
	OD Value	RGR (%)	Toxicity (grade)	OD Value	RGR (%)	Toxicity (grade)	OD Value	RGR (%)	Toxicity (grade)
Control	0.331			0.471			0.581		
0.25	0.325	97.94	1	0.466	98.83	1	0.535	92.07	1
0.5	0.329	99.18	1	0.446	94.59	1	0.541	93.15	1
1	0.340	102.57	0	0.441	93.66	1	0.553	95.24	1
2	0.325	98.00	1	0.467	99.19	1	0.535	92.11	1
4	0.332	100.23	0	0.478	101.42	0	0.541	93.13	1

failed to inhibit the growth of hUC-MSCs, indicating a better biocompatibility of the scaffolds with hUC-MSCs.

### General Situation of the *in vivo* Experiment

All the animals returned to normal diet and activities after 1 d of surgery, and survived until completion of the experiment. There was no swelling, exudation and infection of the wounds.

### Gross Observation of the *in vivo* Experiment

The gross observation was performed after 6 weeks of the surgery. As shown in Figure 6, no obvious inflammatory reaction was observed in the local tissue for all the animals. For group A (Figure 6A), the specimen could be seen well and the large parts of the defects were filled with semi-transparent tissue, which was still not reaching the cartilage surface. The repaired tissue revealed yellow-white appearance with smooth surface and certain elasticity, but it could be distinguished from the surrounding normal cartilage. For group B (Figure 6B), the repair effect of cartilage was not obvious and the boundary between the repaired and the surrounding tissues was clear. The repaired tissue showed gray-white appearance with a rough surface. And most parts of the scaffold were degraded, but no abnormal reaction of the surrounding tissues happened. For group C (Figure 6C), the specimen could also be seen clearly and an

obvious hollow appeared at the defect site. The repaired tissue was of gray-white color with rough surface and surrounded by a small amount of granulation.

### Histological Observation of the *in vivo* Experiment

The histological staining by HE method was further performed to evaluate the effect of PLGA/HAp/Zein scaffolds on cartilage repair. It was found that for group A (Figure 6D) there were plenty of native-like chondrocytes and matrix. Moreover, the cartilage lacuna could be seen, and the chondrocytes were aligned well with slight hyperplasia. For group B (Figure 6E), the number of cells was less than that in group A, and the cells arrangement was irregular with fibrous hyperplasia. For group C (Figure 6F), the hyperplasia of fibrous connect tissue and neovascularization were observed.

## DISCUSSION

Nowadays, the repair of articular cartilage defect is still one of the main clinical problems. Although several methods have been used to repair the damaged articular cartilage, the effects remain not as good as expected. However, in recent years, the emerging tissue engineering has shed light on the repair of articular cartilage defect. Tissue engineering is an interdisciplinary or a multidisciplinary subject,

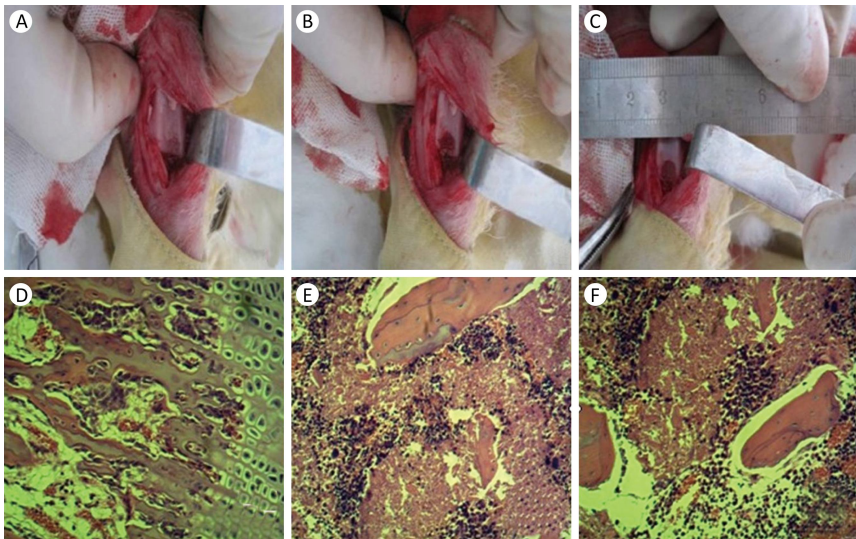


**Figure 6.** Gross (upper) and histological (lower) observation of the cartilage tissue repaired with or without the scaffolds (A, D) hUC-MSCs+ PLGA/HAp/Zein scaffolds; (B, E) PLGA/HAp/Zein scaffolds; (C, F) Control without scaffolds.

including seed cells, scaffolds, and growth factors. Over the past decade, it was found that the MSCs could differentiate to mesoderm cell lines, such as chondrocytes, osteoblasts, adipocytes, cardiac myocytes, and endothelial cells<sup>[23-24]</sup>. hUC-MSCs has been an ideal seed cell for tissue engineered bone-cartilage due to their wide sources, easy obtaining, low immunogenicity, good self-renewal ability, high proliferation efficiency, and multi-differentiation potential. Moreover, the application of hUC-MSCs did not involve social, ethical, legal or other aspects. While for the tissue engineered bone-cartilage scaffolds, the suitable artificial extracellular matrix materials are also necessary except for the seed cells. Generally, the ideal scaffold materials should possess the following properties: good biocompatibility and biodegradability, a certain inductivity and conductivity of bone and cartilage, promoting cell attachment and proliferation, a certain mechanics, good permeability, suitable surface chemical properties and microstructure, forming complexes with other biomolecules and controlled release, easy sterilization. However, up to now, there have been no materials available which possess all the above advantages simultaneously, and this also represents a dilemma for incomplete repair of the cartilage defects by tissue engineered bone-cartilage, especially for the integration of scaffolds with host tissue and mechanical match.

PLGA and HAp are currently the two widely used biomaterials in bone-cartilage tissue engineering as described above. However, few studies refer to the combination of the two biomaterials. Thus, it is interesting to find a suitable method to form PLGA/HAp complexes with complementary properties. In recent years, the electrospun scaffolds have been widely used in various fields of tissue engineering<sup>[25-27]</sup>. The electrospun technique can be used to fabricate fibrous scaffolds with the size in the range from several nanometers to ten micrometers, which could be used to simulate the natural ECM (the diameter of collagen is 50-500 nm). The component of the scaffold materials can be a single polymer or polymer complexes. Moreover, the HAp, growth factors, cell regulation factors, and even living cells could also be embedded in the scaffolds. The scaffolds prepared by electrospun displayed high porosity (about 90%) and better pore connectivity, and the prepared fibers showed extremely large specific surface area, providing better niche for cell survival, which is beneficial for

cell attachment, proliferation, differentiation, and ECM secretion. The degradation ratio of the scaffolds is controllable and the surface could be modified using various physiochemical methods to improve their biocompatibility. In addition, the thickness, components, three-dimensional structure and mechanical properties of the scaffolds by electrospun can also be controlled to obtain different characteristics and functions. Thus, the electrospun technique has attracted ever increasing attention, and various scaffolds fabricated by this method have been widely used in tissue engineering materials, optical or chemical sensors<sup>[28]</sup>, electrode materials<sup>[29]</sup>, drug delivery systems<sup>[30]</sup>, and wound dressing<sup>[31]</sup>. It is reported that the tissue engineering scaffolds fabricated by electrospun have been successfully applied in bone and cartilage tissue engineering. Li and his colleagues<sup>[32-34]</sup> fabricated PLGA nanofibers using electrospun method for cartilage tissue engineering, and found that the PLGA nanofibers possessed suitable porosity and mechanics, and promoted the attachment, proliferation and differentiation of chondrocytes, indicating an useful potential in tissue engineering. Shin et al.<sup>[22]</sup> reported that the mechanics and degradation speed of PLGA nanofibers could be modulated by changing the fabrication parameters. Moreover, the PLGA scaffolds could promote chondrocytes proliferation and ECM formation under intermittent hydrostatic pressure. The growth behavior of MSCs on PLGA nanofibers was also studied by Xin et al.<sup>[35]</sup>, and the SEM findings revealed that the human MSCs and chondroitin derivatives could adsorb on the fibers after 7 d of culture. Then the histological analysis demonstrated that the human MSCs could continue to differentiate to bone and chondrocytes after culture for two weeks. In addition, the adding of inorganic particles such as CaCO<sub>3</sub><sup>[36]</sup> nano HAp<sup>[37-38]</sup> was found to be beneficial for simulating the structure of bone tissue and promoting the repair of cartilage defects.

In this study, the PLGA/HAp/Zein scaffolds were successfully fabricated by electrospun method, and the physiochemical properties of the scaffolds were analyzed by SEM, TEM, and FTIR. Furthermore, the biocompatibility of the scaffolds was evaluated by *in vitro* and *in vivo* experiments. The morphology of the scaffolds and fibers were observed using SEM and TEM, respectively, and it was indicated that the adding of zein could obviously affect the morphology of the prepared scaffolds, which was further verified

by the FTIR characterization. However, many beads appeared on the fibers, which might be ascribed to the low concentration of Zein, while there was too much solvent. Thus, from the results of physiochemical characterization, it was reasonable to believe that only the concentration of Zein was suitable, if an evenly distribution of the fibers could be obtained. The Zein scaffolds has been found to be beneficial for vascularization and tissue regeneration by Tu et al.<sup>[18]</sup>. The aim of Zein addition was anticipated to further promote the formation of bone tissue due to its good biocompatibility, osteogenic activity, biodegradation property and vasoactivity<sup>[18]</sup>. HA and PLGA could be used as the scaffolds parts, moreover, HA could promote osteoblasts differentiation and cartilage development. For the evaluation of biocompatibility, hUC-MSCs were first isolated and identified using flow cytometry. It was found that hUC-MSCs highly expressed MSCs markers (CD105, CD90, CD73), indicating that the isolated cells could be used to evaluate the biocompatibility of the PLGA/HAp/Zein scaffolds. After culturing hUC-MSCs on PLGA/HAp/Zein scaffolds for 1, 3, and 5 d, respectively, we found that the cells could attach and proliferate on the scaffolds well. Moreover, the cells showed pseudopodium on the fibers, indicating a stable attachment on the scaffolds. Then the cytotoxicity and doubling time of hUC-MSCs were evaluated by MTT method, and no obvious difference in cytotoxicity and doubling time was observed compared with the control samples. Thus, the scaffolds possessed good cytocompatibility. Subsequently, the PLGA/HAp/Zein scaffolds with or without hUC-MSCs was implanted into the femurs of rabbits, and after 6 weeks the implants were taken out and analyzed via histological method. The PLGA/HAp/Zein scaffolds with hUC-MSCs could effectively induce the cartilage development. Therefore, the scaffolds may be used as a device for cartilage tissue engineering in the future.

## CONCLUSION

The PLGA/HAp/Zein scaffolds for repairing bone-cartilage defects are successfully fabricated by electrospun method. The prepared scaffolds show porous structure with plenty of fibers, and the fibers are within uniform thickness and crisscross arrangement. In addition, a stable systematic method for isolation, culture and identification of hUC-MSCs is established. The obtained hUC-MSCs

have the properties including high purity, stable biological activity and rapid amplification, etc, which provides the possibility for obtaining excellent seed cells. The results of *in vitro* hUC-MSCs culture on PLGA/HAp/Zein scaffolds show that the cells could attach and proliferate well on the scaffolds, suggesting that the scaffolds is not cytotoxic with good biocompatibility. Then the *in vivo* experiments further demonstrate that PLGA/HAp/Zein scaffolds with hUC-MSCs could induce the formation of cartilage, which is of potential significance for the implantation of biomedical devices in bone-cartilage tissue. Therefore, the present study may offer a potential application of PLGA/HAp/Zein scaffolds in bone-cartilage tissue engineering.

Received: April 14, 2014;

Accepted: July 29, 2014

## REFERENCES

- Grenier S, Bhargava MM, Torzilli PA. An *in vitro* model for the pathological degradation of articular cartilage in osteoarthritis. *J Biomech*, 2014; 47, 645-52.
- Iwamoto M, Ohta Y, Larmour C, et al. Toward regeneration of articular cartilage. *Birth Defects Res C Embryo Today*, 2013; 99, 192-202.
- Becerra J, Andrades JA, Guerado E, et al. Articular cartilage: structure and regeneration. *Tissue Eng Part B*, 2010; 16, 617-27.
- Jurgens WJ, Kroeze RJ, Bank RA, et al. Rapid attachment of adipose stromal cells on resorbable polymeric scaffolds facilitates the one-step surgical procedure for cartilage and bone tissue engineering purposes. *J Orthop Res*, 2011; 29, 853-60.
- Sun H, Liu W, Zhou G, et al. Tissue engineering of cartilage, tendon and bone. *Front Med*, 2011; 5, 61-9.
- Bara JJ, McCarthy HE, Humphrey E, et al. Bone marrow-derived mesenchymal stem cells become antiangiogenic when chondrogenically or osteogenically differentiated: implications for bone and cartilage tissue engineering. *Tissue Eng Part A*, 2014; 20, 147-59.
- Nuernberger S, Cyran N, Albrecht C, et al. The influence of scaffold architecture on chondrocyte distribution and behavior in matrix-associated chondrocyte transplantation grafts. *Biomaterials*, 2011; 32, 1032-40.
- Rodrigues MT, Gomes ME, Reis RL. Current strategies for osteochondral regeneration: from stem cells to pre-clinical approaches. *Curr Opin Biotechnol*, 2011; 22, 726-33.
- Jiang CC, Chiang H, Liao CJ, et al. Repair of porcine articular cartilage defect with a biphasic osteochondral composite. *J Orthop Res*, 2007; 25, 1277-90.
- Li M, Liu W, Sun J, et al. Culturing primary human osteoblasts on electrospun poly(lactic-co-glycolic acid) and poly(lactic-co-glycolic acid)/nanohydroxyapatite scaffolds for bone tissue engineering. *ACS Appl Mater Interfaces*, 2013; 5, 5921-6.
- Jeong SI, Kim SY, Cho SK, et al. Tissue-engineered vascular grafts composed of marine collagen and PLGA fibers using pulsatile perfusion bioreactors. *Biomaterials*, 2007; 28, 1115-22.
- Wan Y, Qu X, Lu J, et al. Characterization of surface property of

- poly(lactide-co-glycolide) after oxygen plasma treatment. *Biomaterials*, 2004; 25, 4777-83.
13. Asaoka T, Ohtake S, Furukawa KS, et al. Development of bioactive porous alpha-TCP/HAp beads for bone tissue engineering. *J Biomed Mater Res A*, 2013; 101, 3295-300.
  14. Dong J, Sun QS, Wang JY. Basic study of corn protein, zein, as a biomaterial in tissue engineering, surface morphology and biocompatibility. *Biomaterials*, 2004; 25, 4691-7.
  15. Liu XM, Sun QS, Wang HJ, et al. Microspheres of corn protein, zein, for an ivermectin drug delivery system. *Biomaterials*, 2005; 26, 109-15.
  16. Gong S, Wang H, Sun Q, et al. Mechanical properties and *in vitro* biocompatibility of porous zein scaffolds. *Biomaterials*, 2006; 27, 3793-9.
  17. Wang HJ, Gong SJ, Lin ZX, et al. *In vivo* biocompatibility and mechanical properties of porous zein scaffolds. *Biomaterials*, 2007; 28, 3952-64.
  18. Tu J, Wang H, Li H, et al. The *in vivo* bone formation by mesenchymal stem cells in zein scaffolds. *Biomaterials*, 2009; 30, 4369-76.
  19. Brenner JM, Ventura NM, Tse MY, et al. Implantation of scaffold-free engineered cartilage constructs in a rabbit model for chondral resurfacing. *Artif Organs*, 2014; 38, E21-32.
  20. Kuo TF, Lin MF, Lin YH, et al. Implantation of platelet-rich fibrin and cartilage granules facilitates cartilage repair in the injured rabbit knee: preliminary report. *Clinics (Sao Paulo)*, 2011; 66, 1835-8.
  21. Han CW, Chu CR, Adachi N, et al. Analysis of rabbit articular cartilage repair after chondrocyte implantation using optical coherence tomography. *Osteoarthritis Cartilage*, 2003; 11, 111-21.
  22. Shin HJ, Lee CH, Cho IH, et al. Electrospun PLGA nanofiber scaffolds for articular cartilage reconstruction: mechanical stability, degradation and cellular responses under mechanical stimulation *in vitro*. *J Biomater Sci Polym Ed*, 2006; 17, 103-19.
  23. Phinney DG, Kopen G, Isaacson RL, et al. Plastic adherent stromal cells from the bone marrow of commonly used strains of inbred mice: variations in yield, growth, and differentiation. *J Cell Biochem*, 1999; 72, 570-85.
  24. Ragni E, Viganò M, Parazzi V, et al. Adipogenic potential in human mesenchymal stem cells strictly depends on adult or foetal tissue harvest. *Int J Biochem Cell Biol*, 2013; 45, 2456-66.
  25. Chen H, Fan X, Xia J, et al. Electrospun chitosan-graft-poly (varepsilon-caprolactone)/poly (varepsilon-caprolactone) nanofibrous scaffolds for retinal tissue engineering. *Int J Nanomedicine*, 2011; 6, 453-61.
  26. Walser J, Caversaccio MD, Ferguson SJ. Electrospinning Auricular Shaped Scaffolds for Tissue Engineering. *Biomed Tech (Berl)*, 2013. doi: <http://dx.doi.org/10.1515/bmt-2013-4203>
  27. Ramachandran K, Gouma PI. Electrospinning for bone tissue engineering. *Recent Pat Nanotechnol*, 2008; 2, 1-7.
  28. Sun B, Long YZ, Liu SL, et al. Fabrication of curled conducting polymer microfibrillar arrays via a novel electrospinning method for stretchable strain sensors. *Nanoscale*. 2013; 5, 7041-5.
  29. Jafari A, Jeon JH, Oh IK. Well-aligned nano-fiberous membranes based on three-pole electrospinning with channel electrode. *Macromol Rapid Commun*, 2011; 32, 921-6.
  30. Hu J, Wei J, Liu W, et al. Preparation and characterization of electrospun PLGA/gelatin nanofibers as a drug delivery system by emulsion electrospinning. *J Biomater Sci Polym Ed*, 2013; 24, 972-85.
  31. Dubsy M, Kubinova S, Sirc J, et al. Nanofibers prepared by needleless electrospinning technology as scaffolds for wound healing. *J Mater Sci Mater Med*, 2012; 23, 931-41.
  32. Li WJ, Danielson KG, Alexander PG, et al. Biological response of chondrocytes cultured in three-dimensional nanofibrous poly(epsilon-caprolactone) scaffolds. *J Biomed Mater Res A*, 2003; 67, 1105-14.
  33. Li WJ, Laurencin CT, Cateson EJ, et al. Electrospun nanofibrous structure: a novel scaffold for tissue engineering. *J Biomed Mater Res*, 2002; 60, 613-21.
  34. Li WJ, Tuli R, Okafor C, et al. A three-dimensional nanofibrous scaffold for cartilage tissue engineering using human mesenchymal stem cells. *Biomaterials*, 2005; 26, 599-609.
  35. Xin X, Hussain M, Mao JJ. Continuing differentiation of human mesenchymal stem cells and induced chondrogenic and osteogenic lineages in electrospun PLGA nanofiber scaffold. *Biomaterials*, 2007; 28, 316-25.
  36. Koo KT, Polimeni G, Qahash M, et al. Periodontal repair in dogs: guided tissue regeneration enhances bone formation in sites implanted with a coral-derived calcium carbonate biomaterial. *J Clin Periodontol*, 2005; 32, 104-10.
  37. Deng XL, Sui G, Zhao ML, et al. Poly(L-lactic acid)/hydroxyapatite hybrid nanofibrous scaffolds prepared by electrospinning. *J Biomater Sci Polym Ed*, 2007; 18, 117-30.
  38. Lee JB, Park HN, Ko WK, et al. Poly(L-lactic acid)/hydroxyapatite nanocylinders as nanofibrous structure for bone tissue engineering scaffolds. *J Biomed Nanotechnol*, 2013; 9, 424-9.